

# Chirped quasi-phase-matching with Gauss sums for production of biphotons

D. A. Antonosyan,<sup>1,2,\*</sup> A. R. Tamazyan,<sup>1,2,†</sup> and G. Yu. Kryuchkyan<sup>1,2,‡</sup>

<sup>1</sup>*Yerevan State University, Alex Manoogian 1, 0025, Yerevan, Armenia*

<sup>2</sup>*Institute for Physical Researches, National Academy of Sciences,  
Ashtarak-2, 0203, Ashtarak, Armenia*

We study the theory of linearly chirped biphoton wave-packets produced in two basic quasi-phase-matching configurations: chirped photonic-like crystals and aperiodically poled crystals. The novelty is that these structures are considered as definite assemblies of nonlinear layers that leads to detailed description of spontaneous parametric down-conversion (SPDC) processes through the discrete Gauss sums. We demonstrate that biphoton spectra for chirped photonic crystals involving a small number of layers consist from definite well-resolved spectral lines. We also discuss the forming of broadband spectra of signal (idler) waves in SPDC for both configurations as number of layers increases as well as in dependence of chirping parameters.

PACS numbers: 42.65.Lm, 42.50.Dv, 42.65.Yj

## I. INTRODUCTION

One of the challenges in the fields of quantum optics and quantum communications is generation of new sources of nonclassical light, such as biphotons with controllable spectral and temporal properties. The standard method for the generation of biphotons is spontaneous parametric down-conversion (SPDC) [1–3], where photon pairs are generated under action of a strong pump field interacting with a nonlinear crystal. In particular, of considerable interest is preparation of biphoton wave-packets with small correlation times between two-photons as well as with broad frequency spectra. Correlated photon pairs with broad spectra are mainly generated by SPDC using method of quasi-phase-matching (QPM) that provides a feasible alternative to conventional phase matching for many optical parametric process applications. Several methods have been suggested and experimentally implemented in this direction for generation of biphotons, including SPDC in aperiodically poled crystals [4–9]. Studies in this direction allow us to understand three-photon interactions at scale of the shortest possible correlation time that is a single optical cycle [8]. Thus, these investigations are interesting from the fundamental point of view as well as are useful for further applications in quantum technologies. QPM leading to photon pair production is effectively realized in layered nonlinear structures, particularly, in periodically-poled second-order crystals or photonic crystals. The applications have been done for synthesis of twin photon states by manipulating overall group delay mismatches between interacting waves in a multilayered structures by using compensating dispersive effects [10–13], for production of entangled three-photon states in cascaded parametric processes [14–16].

As it has been recently experimentally demonstrated

biphotons with broad spectra and ultrashort correlation time at a high emission rate can be generated using chirped QPM nonlinear crystals that involve nonlinear grating in the spatial coordinate along the direction of pump propagation with a nonuniform poling period [17–20]. In this case, phase-matching is achieved along the crystal in such a way that the phase-matching conditions vary longitudinally by use of QPM which leads to broadband biphoton.

The theory of linearly chirped biphoton wave-packets is usually based on simple model allowing analytical description of linearly chirped periodically-poled crystals or optical fibers (see, [17–20]). In this model a phase-matching function of three-wave interaction  $\exp[i\Delta k(z)z]$  with a QPM grating with linearly varying spatial frequency  $\Delta k(z) = \Delta k - \alpha z$  has been considered. The interaction leads to biphoton spectral density in form of the  $\text{erfi}(x)$  error function. Such phenomenological approach qualitatively explains the basis properties of chirped quasi-phase-matching, in this number: extremely wide spectral bandwidths of biphoton wave packets and the sharp temporal separation between the signal and idler photons comprising a pair. However, this approach has been unable to describe some important details of chirped three-wave interactions.

In this paper, we present more detailed description of chirped structures for generation of two-photon light via SPDC from a cw pump in another way: as the definite assembly of nonlinear segments. This approach provides more flexibility for designing of QPM gratings and allows us engineer the controllable phase relation between the various spectral components. On the whole it becomes possible to control the frequencies and bandwidths of the signal and idler photons by varying also the number of layers equally with the local poling period along the length of the crystal. In this approach the total amplitude of two-photon generation is calculated as the superposition of partial amplitudes corresponding to each layer with local spatial chirp frequency. As frequencies of signal and idler photons are varied with different layers a much broader range of photon frequencies is formed due

\*antonosyand@ysu.am

†a.tamazyan@ysu.am

‡kryuchkyan@ysu.am

to the superposition. Such detailed analysis of chirped QPM allows considering interference and transition effects in SPDC stipulated by definite numbers of layers. In this approach the quasi-phase-matching function of SPDC is expressed through so called Gauss sums instead of the continuous error function that is appeared in the phenomenological approach. It should be mentioned that during recent years it has been seen an impressive number of experiments implementing Gauss sums

$$S_N(\zeta) = \sum_{m=-M}^M W_m e^{2\pi i(m + \frac{m^2}{N})\zeta} \quad (1)$$

in physical systems, particularly, for number factorization schemes. These systems range from nuclear magnetic resonance (NMR) methods [21–23] via cold atoms [24] and Bose-Einstein condensates (BECs) [25], tailored ultrashort laser pulses [26, 27] to classical light in a multi-path Michelson interferometer [28, 29] (for an introduction to this field, see [30, 31]). In addition to these results here we present new quantum systems for implementation of Gauss sums to factor numbers.

We investigate two structures: chirped layered photonic crystals and aperiodically poled layered crystals. In the phenomenological approach in which the phase-matching function is described by the continuous error function both structures give the same results distincting only on the physical parameters. However, detailed description of these chirped structures shows important differences between them.

The paper is organized as follows: In Sec. II, the brief description of SPDC in multilayered media is presented. Sec. III is devoted to chirp in layered photonic-like crystals. The production of broadband biphotons in aperiodically poled layered crystals is described in Sec. IV. We summarize our results in Sec. V.

## II. SPDC IN MULTILAYERED MEDIA: BRIEF DESCRIPTION

In this section we briefly describe generation of two-photon light via SPDC in one-dimensional  $\chi^{(2)}$  media consisting of layers with different coefficients of nonlinearity and refractive indices [10], [13], [14]. We consider collinear, type-II QPM configurations for generation of photons at the same frequency. Since the generated photons are collinear, their directions cannot be used to distinguish the two photons. Thus, we assume that photons in pairs have different polarizations, but omit the polarization indexes below. Three-wave interaction Hamiltonian is expressed as the sum of interactions in each layer in terms of the electric fields for the  $m$ -th layer,  $E_{0m}(z, t)$ ,  $E_{jm}^-(z, t)$ ,  $E_{jm}^+(z, t)$ ,  $j=(s, i)$ ,

$$H(t) = \sum_m \int_{z_m}^{z_{m+1}} dz \chi^{(2)}(z) E_{0m}^*(z, t) E_{im}^{(-)}(z, t) E_{sm}^{(-)}(z, t) + h.c. \quad (2)$$

Here  $\chi^{(2)}(z)$  is the second-order susceptibility,  $E_{0m}(z, t)$  represents classical laser field at the frequency  $\omega_0$  and  $E_{im}^{(-)}(z, t)$ ,  $E_{sm}^{(-)}(z, t)$  represent the positive-frequency parts of the fields of the subharmonics centered at the frequencies  $\omega_i = \frac{\omega_0}{2} + \Omega$ ,  $\omega_s = \frac{\omega_0}{2} - \Omega$ .

The two-photon state can be written as

$$|\psi\rangle = \int \int d\omega_s d\omega_i \Phi(\omega_s, \omega_i) a^+(\omega_s) a^+(\omega_i) |0\rangle, \quad (3)$$

where  $a^+(\omega_s)$  and  $a^+(\omega_i)$  are the creation photon operators for modes with frequencies  $\omega_s$  and  $\omega_i$ ,  $\omega_0 = \omega_s + \omega_i$ ,  $|0\rangle$  is a vacuum state of the signal and the idler fields and  $\Phi(\omega_s, \omega_i)$  is the spectral amplitude of two photon radiation. Two-photon amplitude for multilayered structures has been presented in many papers [10], [13], (see, also [14–16]). It has been calculated as the sum of definite partial amplitudes in the general form given by the product of the pump envelope function  $E_0(\omega_0)$  and the phase matching function  $F(\Delta k)$

$$\Phi(\omega_s, \omega_i) = \frac{-2\pi i}{\hbar} E_0(\omega_s + \omega_i) F(\Delta k), \quad (4)$$

$$F = \sum_m l_m \chi_m F_m, \\ F_m = e^{-i(\varphi_m + \frac{\Delta k_m l_m}{2})} \text{sinc}\left(\frac{\Delta k_m l_m}{2}\right) \\ \varphi_m = \sum_n^{m-1} l_n \Delta k_n, \quad \varphi_1 = 0. \quad (5)$$

Here,  $\chi_m$  is the second-order susceptibility in the  $m$ -th layer,  $l_m = z_{m+1} - z_m$  is the length and  $\Delta k_m = k_0^m - k_s^m - k_i^m$  is the phase mismatch vector for the  $m$ -th layer,  $k_j^m(z, \omega_j) = \frac{\omega_j}{c} n_m(z, \omega_j)$ ,  $n_m(\omega)$  is the corresponding refractive index of the medium at the given frequency that describes the effects of dispersion on the properties of photon pairs. In this case the probability of twin-photon generation is calculated as

$$|\Phi(\omega_s, \omega_i)|^2 = \frac{(2\pi)^2}{\hbar^2} |E_0|^2 \times |F|^2, \\ |F|^2 = \sum_{m=1}^N |F_m|^2 + 2 \text{Re} \left( \sum_{m_1 < m_2} F_{m_1} F_{m_2}^* \right) \quad (6)$$

in the form which clearly demonstrates that the interfering probability amplitudes  $A_m \sim E_0 F_m$  of two-photon generation in each layer contribute to the total probability. Further, for convenience we expand the wave vectors in Taylor series around the exact quasi-phase-matching frequency and take into consideration only the zero- and first-order terms:  $k_s = k_s(\frac{\omega_0}{2}) - \Omega k'_s$ ,  $k_i = k_i(\frac{\omega_0}{2}) + \Omega k'_i$ , where  $k'_{i,s}$  are the first derivatives of the dispersion law evaluated at  $\frac{\omega_0}{2}$ , related to the group velocity. This approximation means that the spectrum of biphotons is not too broad compared to the difference of group velocities of the subharmonics.

### III. CHIRP IN PHOTONIC-LIKE CRYSTALS

Recently, non linear photonic crystals have been used in the context of the process of spontaneous parametric down-conversion. In particular, the semiconductor-based nonlinear one-dimensional photonic crystals have been explored for phase-matching in generation of polarization-entangled photon pairs [32], [33]. It has been demonstrated that one-dimensional photonic crystal are very effective for generation of photon pair due to field localization in such structures [34], [35], [36]. The production of photon pairs with engineered spectral entanglement properties in one-dimensional nonlinear photonic crystals has been shown in [37].

In this section, we study one-dimensional nonlinear photonic crystals for chirp configuration. In the scheme proposed generation of photon pairs by SPDC in  $\chi^{(2)}$  layered structure characterized by a chirp in its linear optical properties. Considering the general equation (5), we assume that layers have the equal lengths  $l_m = l$  as well as the equal susceptibilities  $\chi_m = \chi_0$ , while refractive indexes of the pump  $n(\omega_0, z) = n_0(z)$  and the generated waves  $n(\omega_j, z) = n_j(z)$  ( $j = s, i$ ) have linear dependence on the coordinate and are given by

$$\begin{aligned} n_0(z) &= \begin{cases} n_0, & 0 < z < l; \\ n_0 - ml\beta_0, & ml < z < (m+1)l, \end{cases} \\ n_j(z) &= \begin{cases} n_j, & 0 < z < l; \\ n_j - ml\beta_j, & ml < z < (m+1)l, \end{cases} \end{aligned} \quad (7)$$

where  $\beta_0$  and  $\beta_j$  ( $j = s, i$ ) are chirp parameters for the

refractive indexes of the pump and subharmonic waves, correspondingly. In this case, the phase-mismatch vector for the  $m$ -th layer has a linear chirp of the following form  $\Delta k_m = \Delta k - \alpha(m-1)l$ , where  $\Delta k = k_0(\omega_0) - k_s(\omega_s) - k_i(\omega_i)$  is the phase mismatch vector at the first layer, and  $\alpha = \frac{\omega_0}{c}(\beta_0 - \frac{\beta_s}{2} - \frac{\beta_i}{2})$  is the spatial chirp parameter.

Taking into account (7) we present the general expression (5) as

$$\begin{aligned} F(\Delta k) &= l\chi_0 e^{i\frac{l\Delta k}{2}} \sum_{m=1}^N F_m, \\ F_m &= e^{-i(ml\Delta k - \frac{\alpha(m-1)^2 l^2}{2})} \times \text{sinc}\left(\frac{(\Delta k - \alpha(m-1)l)l}{2}\right), \end{aligned} \quad (8)$$

where  $\text{sinc}(x) = \frac{\sin(x)}{x}$ .

It is easy to see that in the frame of this presentation, the phase matching function is given by the Gauss sum, in spite of the error functions that are appeared in the phenomenological approach [8, 18]. Below, we calculate these sums considering the phase-mismatch function as  $\Delta k = \Delta k_0 + \Omega D$ , where  $\Delta k_0 = k_0 - k_s(\frac{\omega_0}{2}) - k_i(\frac{\omega_0}{2})$  and  $D = k'_s - k'_i$  is temporal walkoff between signal and idler modes, assuming that  $\Delta k_0$  satisfies the QPM condition. In order to illustrate the broadening of the spectrum and the other features of obtained phase-matching function we have calculated the squared amplitude of the phase-matching function  $|F(\Omega)|^2$  on the base of the formula (6) and the wave vector dispersion expansion as

$$\begin{aligned} |F(\Omega)|^2 &= l^2 \chi_0^2 \left[ \sum_{m=1}^N \text{sinc}^2\left(\frac{(D\Omega + \Delta k_0 - \alpha(m-1)l)l}{2}\right) + 2 \sum_{m=1}^{N-1} \sum_{p=1}^{N-m} \left( \text{sinc}\left(\frac{(D\Omega + \Delta k_0 - \alpha(m-1)l)l}{2}\right) \times \right. \right. \\ &\quad \left. \left. \times \text{sinc}\left(\frac{(D\Omega + \Delta k_0 - \alpha(m+p-1)l)l}{2}\right) \right) \cos\left(p(D\Omega + \Delta k_0)l - \alpha p\left(m-1 - \frac{p}{2}\right)l^2\right) \right]. \end{aligned} \quad (9)$$

We present a detailed analysis of normalized biphoton spectral density  $|f|^2 = \frac{|F|^2}{L^2 \chi_0^2}$  in dependence on the wavelength of signal (idler) mode. In this way, we select in the Fig. (1) the results for typical values of pump wave length  $\lambda_0 = 0.458 \mu\text{m}$ , the chirp parameter  $\alpha = 1200 \text{cm}^{-2}$ ,  $B = cD = 0.3$  and crystal with the total length  $L = 0.8 \text{cm}$  taken from the experimental results on LiTaO<sub>3</sub> [18]. Note, that our approach allows to consider the general case of arbitrary number of layers on the base of the formula (9). To develop comparatively analysis we represent the squared amplitude of the phase matching function for the crystals with the fixed total length  $L$ , but with the various number of domains, particularly, for the

cases of small and large numbers of layers.

The results are depicted in Figs.1(a,b) for  $N = 5$  and  $N = 10$  layers and the phase-matching conditions  $\Delta k_0 = 3\alpha l$  and  $\Delta k_0 = 5\alpha l$ , correspondingly. As we see, in these cases the biphoton spectra consist from definite separated spectral peaks corresponding to the number of domains. The frequencies of the spectral lines are given by  $\Omega_m = [\alpha(m-1)l - \Delta k_0]D^{-1}$  according to the formula (9) provided that the spectral lines are resolved i.e. their widths are less than the intervals between them in the range of the wave-length broadening. Thus, there are critical ranges of domains number when the spectral lines are not resolved and chirp leads to the broadening of the

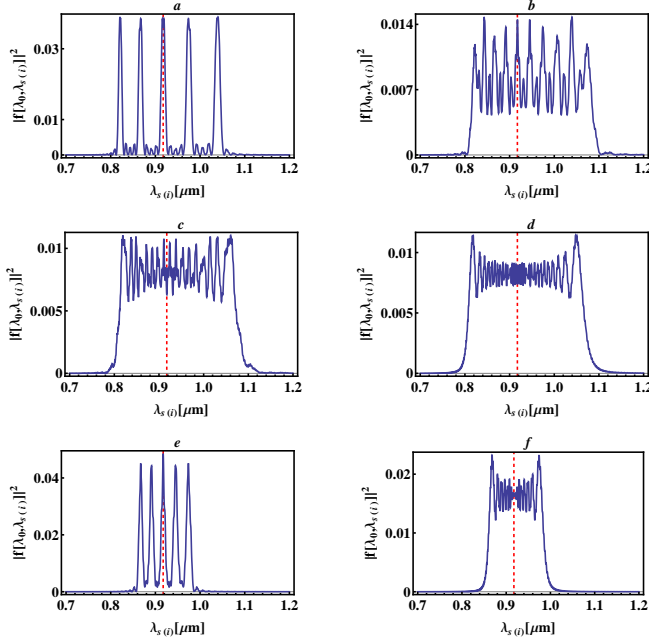


FIG. 1: Biphoton spectral density in dependence on the wavelengths of signal (idler) field for the crystals with the length  $L = 8000\mu\text{m}$ , dispersion parameter  $B = 0.3$ , chirp parameter  $\alpha = 1.2 \times 10^{-5}\mu\text{m}^{-2}$  and different numbers of layers:  $N = 5$ ,  $\Delta k_0 = 3\alpha l$  (a);  $N = 10$ ,  $\Delta k_0 = 5\alpha l$  (b);  $N = 20$ ,  $\Delta k_0 = 10\alpha l$  (c) and  $N = 80$ ,  $\Delta k_0 = 40\alpha l$  (d). The cases of the chirping parameter  $\alpha = 6 \times 10^{-6}\mu\text{m}^{-2}$ :  $N = 5$ ,  $\Delta k_0 = 3\alpha l$  (e);  $N = 80$ ,  $\Delta k_0 = 40\alpha l$ , (f). The red dashed lines correspond to the wavelength  $2\lambda_0 = 0.916\mu\text{m}$ .

biphoton spectra.

If domains' number is increasing, the chirp is displayed as a broadening of the biphoton spectra as it is depicted in Figs.1(c,d) for  $N = 20$  and  $N = 80$  layers and the phase-matching conditions  $\Delta k_0 = 10\alpha l$  and  $\Delta k_0 = 40\alpha l$ , respectively. One can see that the spectrum of the biphoton field is quite broad (from 900 nm to 1300 nm wavelength) and has nearly rectangular shape already for  $N = 80$  (see, Fig. 1(d)). For further increasing of the number of domains the interference picture become smooth and the results qualitatively coincidence with the analogous results obtained on the base of simple model [17, 18].

It should be noted that the length of biphoton spectral shape does not depend from the number of layers for fixed

total length of nonlinear media but is only determined by the chirping parameter. We illustrate this statement on Fig.1 (e,f) by consideration of the other chirping parameter  $\alpha = 0.000006\mu\text{m}^{-2}$  that is two times less than the previous one, for  $N=5$  and  $N=80$  layers, correspondingly. As we see, increasing of the chirping parameter leads to the increase of the intervals between the spectral peaks for the case of small numbers of layers. For the case of large layers' numbers this increasing leads to the increase of the range of the wave-length spectral broadening.

#### IV. CHIRP IN APERIODICALLY POLED CRYSTALS

Recently, a aperiodic poling have been used for various applications. It has been provided not only for compensation of a natural phase mismatch but has been allowed to tailor the properties of emitted photon pairs using nonlinear domains with variable lengths (chirped periodical poling). Domains of different lengths in an ordered structure allow an efficient nonlinear interaction in an ultra-wide spectral region extending typically over several hundreds of nm [4–9, 38, 39]. It has been shown that photon pairs generated in such structures can posses quantum temporal correlations at the timescale of fs. Other applications of ultra-wideband biphotons include nonclassical metrology [40] and large bandwidth quantum information processing [41], [42].

We consider aperiodically poled crystals as a multilayered structure consisting of  $N$  layers with variation of lengths: the length of each layer is larger from the previous by a chirp parameter  $\zeta$ . So the length of  $n$ -th layer is given by the following expression  $l_n = l_0 + (n - 1)\zeta$ , where  $l_0$  is the length of the first layer. We consider the quadratic nonlinearity  $\chi_n$  having a constant  $\chi_n = (-1)^{(n-1)}\chi_0$  value within each  $n$ -th layer. This structure can be divided into  $N/2$  domains such that each of them will be consist of two layers with reversed crystal axes. So the poling period  $\Lambda$  which is the length of the domain races by  $2\zeta l$  for any next domain, which means it is dependent on the coordinate. Thus, it is easy to realize that the relation between chirp parameters  $\zeta$  and  $\alpha$  can be written as follows  $\zeta = \frac{\alpha l_0^2}{\pi}$ .

According to the formulas (5) we obtain two-photon spectral amplitude  $F(\Delta k)$  for the case of aperiodically poled crystal in the following form

$$F(\Delta k) = \frac{\chi_0}{\Delta k} \exp\left(-i\frac{\Delta k l_0}{2}\right) \sum_{m=1}^M (-1)^m \exp\left(-i\Delta k \left(ml_0 + \frac{(m-1)^2\zeta}{2}\right)\right) \sin\left(\frac{\Delta k(l_0 + (m-1)\zeta)}{2}\right), \quad (10)$$

through the discrete Gauss sum, where  $\Delta k$  is the phase mismatch function. In this case the probability of bipho-

ton generation as a function of the frequency  $\Omega$  is pro-

portional to

$$|F(\Omega)|^2 = \frac{\chi_0^2}{(D\Omega + \Delta k_0)^2} \left[ \sum_{m=1}^N \sin^2 \left( (D\Omega + \Delta k_0) \frac{(l_0 + \zeta(m-1))}{2} \right) + 2 \sum_{m=1}^{N-1} \sum_{p=1}^{N-m} (-1)^p \times \right. \\ \left. \times \sin \left( (D\Omega + \Delta k_0) \frac{(l_0 + \zeta(m+p-1))}{2} \right) \sin \left( (D\Omega + \Delta k_0) \frac{(l_0 + \zeta(m-1))}{2} \right) \cos \left( p(D\Omega + \Delta k_0) \left( l_0 + \frac{\zeta(2m+p-2)}{2} \right) \right) \right]. \quad (11)$$

Here  $\Delta k_0 = k_i(\frac{\omega_0}{2}) + k_s(\frac{\omega_0}{2}) - k_0$  is the phase mismatch vector at the central idler and signal frequencies  $\omega_i = \omega_s = \frac{\omega_0}{2}$ , where  $\omega_0$  is the laser pump frequency. In this formula we have considered also  $\Delta k = \Delta k_0 + D\Omega$ .

It is easy to realize that the biphoton spectra for two systems under consideration are essentially different in form. The main difference is that biphoton spectra for aperiodically poled structures do not consist from separated spectral peaks in the case of small layers in opposite to the case of photonic crystal. If the chirp parameter  $\zeta$  equals to zero the spectrum (11) is reduced to the spectral function of biphotons for pure periodically poled configuration that includes segments of length  $l_0$  with positive  $\chi_0$  and negative  $-\chi_0$  susceptibilities that alternate one to the other

$$|F(\Omega)|^2 = l_0^2 \chi_0^2 \frac{\sin^2 \left( \frac{(D\Omega + \Delta k_0 - \frac{\pi}{l_0})l_0}{2} \right)}{\sin^2 \left( \frac{(D\Omega + \Delta k_0 - \frac{\pi}{l_0})l_0}{2} \right)} \text{sinc}^2 \left( \frac{(D\Omega + \Delta k_0)l_0}{2} \right) \quad (12)$$

In the approximation  $N \gg 1$  this probability reads as  $F|\Omega|^2 \sim l_0^2 N^2 \text{sinc}^2 \left( \frac{l_0(D\Omega + \Delta k_0)}{2} \right)$ . We illustrate the peculiarities of the biphoton spectra in dependence on  $\Omega$  for aperiodically poled structure as well as for periodically poled structure on Figs. 2 for  $N = 50$  and  $\Delta k_0 = 0$ . As we see, in the limit  $\zeta = 0$  and  $N \gg 1$  there occur only one narrow pick for positive  $\Omega$  centered at  $\frac{\pi}{l_0}$ . Increasing of the chirp parameter broadens the frequency spectrum.

Typical biphoton spectra for aperiodic, chirped poling are shown in Figs. 3 in dependence on the signal-field (idler-field) wavelength ( $\lambda_s \gtrsim 2\lambda_0$ ) for various layer numbers and chirping parameters. For comparison of these spectra with analogous results obtained for the case of photonic crystals as well as with the experimental results (see, for example, [18]) we use the parameters that are suitable for the LiTaO<sub>3</sub> aperiodically poled crystal, with  $B = 0.3$ , the whole length  $L = 0.8\text{cm}$  and for the laser pump frequency  $\lambda_0 = 0.458\mu\text{m}$ .

Biphoton spectral density for an aperiodically poled crystal with layers number  $N=50$ , chirp parameter  $\zeta = 1$  and  $l_0 = 109.5$ , which corresponds to a smaller spatial chirp parameter  $\alpha = 240\text{cm}^{-2}$  is shown in the Fig. 3(a). The analogous result for the case of crystal with the same number of layers, but with chirp parameter  $\zeta = 2.82$  and  $l_0 = 88.09$ , which corresponds to the spatial chirp pa-

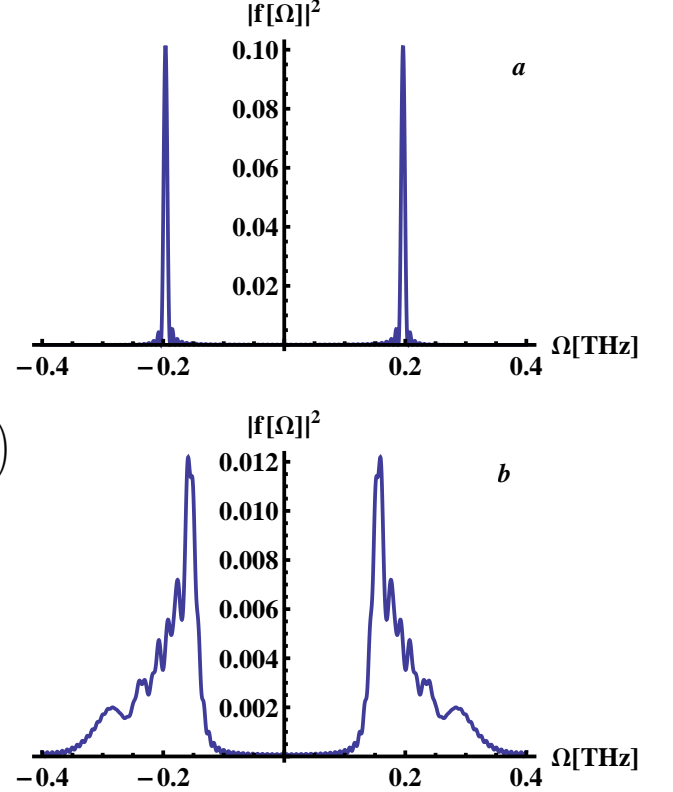


FIG. 2: Biphoton spectra in dependence on  $\Omega$  frequency for non-chirped QPM grating ( $\zeta = 0$ ,  $l = 160\mu\text{m}$  (a)) and chirped QPM grating ( $\zeta = 2.82$ ,  $l_0 = 88.09\mu\text{m}$  (b)). The parameters are:  $L = 8000\mu\text{m}$ ,  $\lambda_0 = 0.458\mu\text{m}$ ,  $B = 0.3$ ,  $N = 50$ .

rameter  $\alpha = 1200\text{cm}^{-2}$  is shown in Fig. 3(b). From comparison of these two results we can see that increasing of chirp parameter on two times lead to wide broadening of the signal- and idler-field spectra. Moreover, for each number of layers there is an optimal value of chirp parameter for which the spectrum is the broadest. In Fig. 3(b,c,d), we show the results of forming the biphoton spectra as number of layer increases provided that the chirping parameter is fixed. For this goal we consider the number of layers:  $N = 50$ ,  $N = 100$

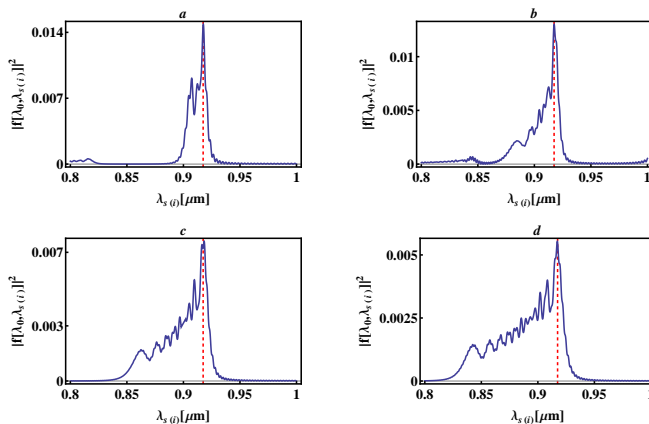


FIG. 3: Biphoton spectral densities in dependence on wavelength for aperiodically poled crystals with the following parameters:  $N = 50$ ,  $l_0 = 109.5\mu\text{m}$ ,  $\zeta = 1\mu\text{m}$ ,  $\Delta k_0 = \frac{\pi}{l_{37}}$  (a);  $N = 50$ ,  $l_0 = 88.09\mu\text{m}$ ,  $\zeta = 2.82\mu\text{m}$ ,  $\Delta k_0 = \frac{\pi}{l_{40}}$  (b);  $N = 100$ ,  $l_0 = 52.225\mu\text{m}$ ,  $\zeta = 0.55\mu\text{m}$ ,  $\Delta k_0 = \frac{\pi}{l_{85}}$  (c);  $N = 160$ ,  $l_0 = 35.51\mu\text{m}$ ,  $\zeta = 0.18\mu\text{m}$ ,  $\Delta k_0 = \frac{\pi}{l_{140}}$  (d). Here  $l_n = l_0 + n\zeta$  and  $B = 0.3$ ,  $\lambda_0 = 0.458\mu\text{m}$  and red dashed lines correspond to the wavelength  $2\lambda_0$

and  $N = 160$  and the chirping parameters are chosen so that again  $\alpha = 1200\text{cm}^{-2}$ . As we can see from these pictures the spectra in these three cases have approximately the same form and they qualitatively match with the result for the biphoton spectra broadening presented in [19] but are different in details. The wider broadening occurs for the higher number of layers: for the number of layers  $N = 160$  the spectral width achieves  $0.2\mu\text{m}$ . Thus, we conclude that for the case of aperiodic chirping the width of spectrum is strongly dependent on the number of layers despite the refractive index frequency chirp considered in the previous section. We also observe that in

the case of aperiodically poled crystals the spectral lines corresponding definite segments are not resolved as it is demonstrated in the case of photonic crystals.

## V. CONCLUSION

In conclusion, we have investigated production of biphoton wave packet in two chirped QPM structures presented as the ensemble of second-order nonlinear layers. In this approach the total amplitude of two-photon generation has been calculated as the superposition of partial amplitudes corresponding to each layer with local spatial chirp frequency. In this way, the spectrum of spontaneously generated chirped photons has been calculated through Gauss sums that involve realistic parameters of three-wave interaction in each layers. The detailed calculations have been done for two QPM structures: (a) chirped nonlinear one-dimensional multi-layered photonic crystals; (b) aperiodic poled one-dimensional multi-layered crystals. The advantage of the presented approach is that we have found out clear and easy correlation between number of layers the crystal consists of and the formation of broadband interference shape of the biphoton spectral rate. The physical mechanism of chirping for both structures have been also explained for physically realised parameters. This approach allows us to consider the case of small number of layers. Particularly, it has been demonstrated that biphoton spectra for chirped photonic crystals with small number of layers ( $N=5,10$ ) consist from well-resolved spectral lines. It has been demonstrated two mechanisms for forming the broadband spectra of signal (idler) waves in SPDC for both configurations as number of layers increases and for various chirping parameters.

- 
- [1] S. E. Harris, M. K. Oshman and R. L. Byer, Phys. Rev. Lett. 18, 732 (1967); R. L. Byer and S. E. Harris, Phys. Rev. 168, 1064 (1968).
  - [2] D. Magde and H. Mahr, Phys. Rev. Lett. 18, 905 (1967); D. N. Klyshko and D. P. Krindach, Zh. Eksp. Teor. Fiz. 54, (1968) [Sov. Phys. JETP 27, 371 (1968)].
  - [3] Y. Shih, Rep. Prog. Phys. 66, 1009 (2003).
  - [4] S. Carrasco, J. P. Torres, L. Torner, A. Sergienko, B. Saleh and M. Teich, Opt. Lett. 29, 2429 (2004).
  - [5] S. Carrasco et al., Phys. Rev. A 70, 043817 (2004); Phys. Rev. A 73, 063802 (2006); Opt. Lett. 31, 253 (2006).
  - [6] M. B. Nasr et al., Opt. Commun. 246, 521 (2005).
  - [7] K. A. O'Donnell and A. B. U'Ren, Opt. Lett. 32, 817 (2007).
  - [8] S. E. Harris, Phys. Rev. Lett. 98, 063602 (2007); S. E. Harris and S. Sensarn, in Proceedings of the Ninth Rochester Conference on Coherence and Quantum Optics (CQ09) (OSA, Washington, DC, 2007), paper CMD1.
  - [9] J. Svozilík and J. Peřina Jr., Phys. Rev. A 80, 023819 (2009).
  - [10] D. N. Klyshko, JETP 77, 222 (1993).
  - [11] A. F. Abouraddy, M. B. Nasr, B. E. A. Saleh, A. V. Sergienko and M. C. Teich, Phys. Rev. A 65, 053817(2002).
  - [12] G. DiGiuseppe, M. Atature, M. D. Shaw, A. V. Sergienko, B. E. A. Saleh and M. C. Teich, Phys. Rev. A 66, 013801 (2002).
  - [13] A. B. U'Ren, R. K. Erdmann, M. de la Cruz-Gutierrez and I. A. Walmsley, Phys. Rev. Lett. 97, 223602 (2006).
  - [14] D. A. Antonosyan, and G. Yu. Kryuchkyan, "Modern Optics and Photonics: Atoms and Structured Media", World Scientific Publishing Co.,131-150, (2010).
  - [15] D. A. Antonosyan, T. V. Gevorgyan and G. Yu. Kryuchkyan, Phys. Rev. A 83, 043807 (2011).
  - [16] D. A. Antonosyan and G. Yu. Kryuchkyan, Opt. Com., 285, 795 (2012).
  - [17] M. B. Nasr, S. Carrasco, B. E. A. Saleh, A. V. Sergienko, M. C. Teich, J. P. Torres, L. Torner, D. S. Hum and M. M. Fejer, Phys.Rev.Lett. 100, 183601 (2008).

- [18] G. Brida, M. V. Chekhova, I. P. Degiovanni, M. Genovese, G. Kh. Kitaeva, A. Meda and O. A. Shumilkina, *Phys. Rev. Lett.* 103, 193602 (2009).
- [19] S. Sensarn, G. Y. Yin and S. E. Harris, *Phys. Rev. Lett.* 104, 253602 (2010).
- [20] G. Imeshev, M. A. Arbore, M. M. Fejer, A. Galvanauskas, M. Fermann and D. Harter, *J. Opt. Soc. Am. B* 17, 304 (2000).
- [21] M. Mehring, K. Müller, Averbukh I. Sh., W. Merkel and W. Schleich, *Phys. Rev. Lett.* 98 120502 (2007).
- [22] T. Mahesh, N. Rajendran, X. Peng and D. Suter, *Phys. Rev. A* 75 062303 (2007).
- [23] X. Peng and D. Suter, *Europhys. Lett.* 84 40006 (2008).
- [24] M. Gilowski, T. Wendrich, T. Müller, C. Jentsch, W. Ertmer, E. M. Rasel and W. P. Schleich, *Phys. Rev. Lett.* 100 030201 (2008).
- [25] M. Sadgrove, S. Kumar and K. Nakagawa, *Phys. Rev. Lett.* 101 180502 (2008); *Phys. Rev. A* 79 053618 (2009).
- [26] D. Bigourd, B. Chatel, W. P. Schleich and B. Girard, *Phys. Rev. Lett.* 100 030202 (2008).
- [27] S. Weber, B. Chatel and B. Girard, *Europhys. Lett.* 83 34008 (2008).
- [28] V. Tamma, H. Zhang, X. He, A. Garruccio and Y. Shih, *J. Mod. Opt.* 56 2125 (2009).
- [29] V. Tamma, H. Zhang, X. He, A. Garruccio, W. P. Schleich and Y. Shih, *Phys. Rev. A* 83 020304 (2011).
- [30] S. Wölk, W. Merkel, W. P. Schleich, I. Sh. Averbukh and B. Girard, *New J. Phys.* 13 103007 (2011).
- [31] W. Merkel, S. Wölk, W. P. Schleich, I. Sh. Averbukh, B. Girard and G. G. Paulus, *New J. Phys.* 13 103008 (2011).
- [32] M. J. A. de Dood, W. T. M. Irvine and D. Bouwmeester, *Phys. Rev. Lett.* 93, 040504 (2004).
- [33] W. T. M. Irvine, M. J. A. de Dood and D. Bouwmeester, *Phys. Rev. A* 72, 043815 (2005).
- [34] M. Centini, J. Perina Jr., L. Sciscione, C. Sibilial, M. Scalora, M. J. Bloemer and M. Bertolotti, *Phys. Rev. A* 72, 033806 (2005).
- [35] J. Perina Jr., M. Centini, C. Sibilial, M. Bertolotti and M. Scalora, *Phys. Rev. A* 73, 033823 (2006).
- [36] A. N. Vamivakas, Bahaa E. A. Saleh, Alexander V. Sergienko and Malvin C. Teich, *Phys. Rev. A* 70, 043810 (2004).
- [37] M. Corona and A. B. U'Ren, *Phys. Rev. A* 76, 043829 (2007).
- [38] M. F. Saleh, B. E. A. Saleh and M. C. Teich, *Phys. Rev. A* 79, 053842 (2009).
- [39] T. S. Humble and W. P. Grice, *Phys. Rev. A* 75, 022307 (2007).
- [40] V. Giovannetti, S. Lloyd and L. Maccone, *Phys. Rev. Lett.* 96, 010401 (2006).
- [41] I. A. Khan and J. C. Howell, *Phys. Rev. A* 73, 031801(R) (2006).
- [42] C. K. Law, I. A. Walmsley and J. H. Eberly, *Phys. Rev. Lett.* 84, 5304 (2000).